

Orthonormal bases of extreme spin coherence

Marcin Rudziński,^{1,2} Adam Burchardt,³ and Karol Życzkowski^{1,4}

¹*Faculty of Physics, Astronomy and Applied Computer Science, Jagiellonian University,
ul. Łojasiewicza 11, 30-348 Kraków, Poland*

²*Doctoral School of Exact and Natural Sciences, Jagiellonian University,
ul. Łojasiewicza 11, 30-348 Kraków, Poland*

³*QuSoft, CWI and University of Amsterdam, Science Park 123, 1098 XG Amsterdam, the Netherlands*

⁴*Center for Theoretical Physics, Polish Academy of Sciences, Al. Lotników 32/46, 02-668 Warszawa, Poland*

Spin anticoherent states acquired recently a lot of attention as the most "quantum" states. Some coherent and anticoherent spin states are known as optimal quantum rotosensors. In this work we introduce a measure of spin coherence for orthonormal bases, determined by the average anticoherence of individual vectors, and identify the most and the least coherent bases which lead to orthogonal measurements of extreme coherence. Their symmetries can be revealed using the Majorana stellar representation, which provides an intuitive geometrical representation of a pure state by points on a sphere. Results obtained lead to maximally (minimally) entangled bases in the $2j + 1$ dimensional symmetric subspace of the 2^{2j} dimensional space of quantum states of multipartite systems composed of $2j$ qubits.

I. INTRODUCTION

Geometric methods play an essential role while studying physical systems in classical mechanics [1, 2], relativity [3], quantum mechanics [4, 5], and quantum field theory [6]. The stellar representation, also called *the Majorana representation*, is one of the important geometrical representations in quantum mechanics [7]. The stellar representation presents a spin- j pure state in $N = 2j + 1$ dimensional Hilbert space as a collection of $2j$ points on a sphere. The same constellation represents a symmetric state of a system consisting of $2j$ qubits. In the case of a spin- $\frac{1}{2}$ particle, it reduces to the celebrated Bloch representation of a two-level quantum system (qubit). This representation is used in various contexts such as spinor Bose gases [8–11], entanglement classification in multiqubit systems [12–19], the Berry phase associated with the cyclic evolution of the state [21–23], investigating Lipkin-Meshkov-Glick model [24, 25] and studying symmetries and properties of spin states [26–41].

The Majorana representation appears naturally in the context of $SU(2)$ coherent, and anticoherent states of a given spin j [26–31]. Note that the spin coherence is not basis dependent. Properties of the coherent state $|\mathbf{n}\rangle$ of spin j closely resemble the classical state of spin j pointing in the direction given by vector \mathbf{n} . Hence, in the Majorana representation, the most coherent state is represented by one $2j$ -degenerated point on a sphere. On the other hand, the anticoherent state $|\psi\rangle$ should "point nowhere", and be represented as $2j$ points equally distributed on a sphere [39–41]. However, even if the polarization (coherence) disappears, the higher moments of coherence might not vanish. Hence, anticoherence is defined up to some order [26]. Highly anticoherent states turned out to be applicable as optimal quantum rotosensors [32–35] and are related to spherical t -designs [36–38]. Experimental realization of some of those states was discussed in [42]. The Majorana representation has proven to be a suitable tool to study properties of anticoherent states.

As much as the construction of coherent states is

straightforward, it is not possible to construct an orthonormal basis composed only of coherent states. Furthermore, much effort has been made to determine quantum states with the highest possible anticoherence, while the concept of the most anticoherent, orthonormal basis of states is largely unexplored.

The main goal of this paper is to address the problem of finding the most coherent and the most anticoherent (the least coherent) orthonormal basis of quantum states that provide orthogonal quantum measurements of extreme spin coherence.

To highlight the symmetries that arise in the studied quantum structures, we use the Majorana stellar representation. The constellations representing the bases and vectors obtained in this study exhibit classical symmetries, such as a Platonic solid, its compound, or an Archimedean solid. Geometric configurations of Platonic solids appear in many areas of quantum information theory. In particular, where recently used to construct particular classes of quantum measurements [43, 44], absolutely maximally entangled (AME) states [45] and Bell inequalities [46, 47].

This work is organized as follows. Section II recalls the Majorana representation for both for spin- j state or a symmetric state of $2j$ qubits. Section III presents the measure of coherence of an orthonormal bases, defined using an anticoherence measure initially introduced for quantum states [31]. Section IV describes our methods of searching for the most coherent and anticoherent orthonormal bases and presents the obtained results. Bases of extreme entanglement in the symmetric subspace of $2j$ -qubit systems are discussed in Section V.

II. THE STELLAR REPRESENTATION

The Bloch sphere is a geometrical representation of pure states of a two-level quantum system, often called a qubit. In particular, a state of spin- $\frac{1}{2}$ quantum system, can be naturally represented as a point

on the sphere. Indeed, a pure quantum state

$$Z_0 |\frac{1}{2}, \frac{1}{2}\rangle + Z_1 |\frac{1}{2}, -\frac{1}{2}\rangle, \quad |Z_0|^2 + |Z_1|^2 = 1 \quad (1)$$

uniquely determines a complex number $z = Z_1/Z_0$ (possibly $z = \infty$), which can be projected onto the surface of a 2-dimensional sphere by the stereographic projection:

$$z \mapsto (\theta, \phi) := (2 \arctan|z|, \arg(z)), \quad (2)$$

where $\theta \in [0, \pi]$ and $\phi \in [0, 2\pi]$ are usual spherical coordinates. Note that the stereographic projection provides a bijection between extended complex plane $\mathbb{C} \cup \{\infty\}$ and the surface of the sphere, the reverse transformation is given by $z = e^{i\phi} \tan(\theta/2)$. Furthermore, a complex number z uniquely defines the quantum state (1) satisfying the property $z = Z_1/Z_0$.

In 1932 Ettore Majorana generalized the celebrated Bloch representation for arbitrary spin- j states [7]. The *stellar representation* maps a spin- j state $|\psi\rangle$ from $(2j+1)$ -dimensional Hilbert space \mathcal{H}_{2j+1} into a constellation of $2j$ points on a sphere. More precisely, any spin- j state might be expressed in the angular momentum basis J_z as

$$|\psi\rangle = \sum_{m=-j}^j Z_{j-m} |j, m\rangle \in \mathcal{H}_{2j+1}, \quad (3)$$

where $\sum_{m=-j}^j |Z_{j-m}|^2 = 1$. The state coefficients are further used to construct the *Majorana polynomial* of degree $2j$ in complex variable z ,

$$w(z) = \sum_{k=0}^{2j} (-1)^k Z_k \sqrt{\binom{2j}{k}} z^{2j-k}. \quad (4)$$

Aforesaid polynomial uniquely determines $2j$ possibly degenerated roots z_i , $i = 1, \dots, 2j$, which can be mapped on a sphere by the stereographic projection (2). In this way, the state (3) is represented as $2j$ points on a sphere, which are called *stars*. We refer to such a collection of $2j$ stars written in the spherical coordinates $\{\theta_k, \phi_k\}_{k=1}^{2j}$ as the Majorana representation of a state $|\psi\rangle$, and denote it by

$$\mathcal{M}(|\psi\rangle) := \{\theta_k, \phi_k\}_{k=1}^{2j}. \quad (5)$$

For example, the state $|j, j\rangle$ corresponds to the trivial Majorana polynomial $w(z) = z^{2j}$, which has $2j$ -degenerated root at $z = 0$, and hence is represented by $2j$ stars at the north pole. More generally, the Majorana polynomial corresponding to $|j, m\rangle$ state has two degenerated roots at $z = 0$ and $z = \infty$ with multiplicities $j+m$ and $j-m$ respectively. Hence the state $|j, m\rangle$ is represented by $j+m$ stars at the north and $j-m$ stars at the south pole. Note that for a spin- $\frac{1}{2}$ particle, the Majorana representation, reduces to the Bloch representation of a state provided in (1).

A The stellar representation for symmetric states

The stellar representation has a natural interpretation while identifying a spin- j system with a symmetric subspace of a system of $2j$ qubits. The symmetric

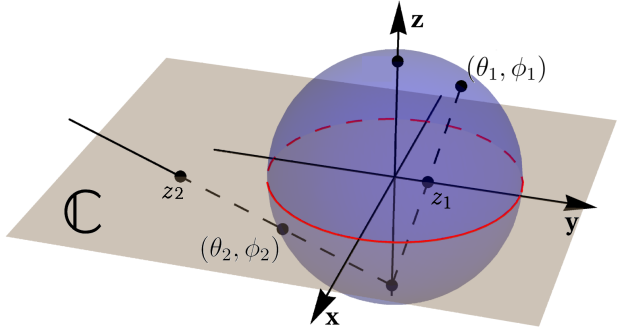


FIG. 1: A sphere with the stereographic projection of points $z_1 = e^{i\phi_1} \tan(\theta_1/2)$ and $z_2 = e^{i\phi_2} \tan(\theta_2/2)$ presented.

subspace of dimension $2j+1$ is spanned by the *Dicke states* $|D_{2j,k}\rangle$, which are a uniform superposition of states with a given number of k excitations [48]

$$|D_{2j,k}\rangle = \binom{2j}{k}^{-\frac{1}{2}} \sum_{\sigma \in \mathbb{S}_{2j}} \sigma(|0\rangle^{\otimes 2j-k} \otimes |1\rangle^{\otimes k}), \quad (6)$$

where $\sigma \in \mathbb{S}_{2j}$ denotes a permutation of subsystems determined by an element of the symmetric group \mathbb{S}_{2j} . Any symmetric state may be uniquely expressed as a combination of Dicke states,

$$|\psi_{sym}\rangle = \sum_{k=0}^{2j} Z_k |D_{2j,k}\rangle \in \mathcal{H}_2^{\otimes 2j}, \quad (7)$$

with normalization $\sum_{k=0}^{2j} |Z_k|^2 = 1$. By identifying the eigenstates of the J_z operator with Dicke states

$$F : |j, m\rangle \mapsto |D_{2j,j-m}\rangle, \quad (8)$$

one can relate a \mathcal{H}_{2j+1} state space with symmetric subspace of $\mathcal{H}_2^{\otimes 2j}$, and hence a spin- j particle with a symmetric state of $2j$ qubits, see Eqs. (3) and (7). Above equation determines the isomorphism F of two spaces, and for any spin- j state $|\psi\rangle$ we denote by $|F(\psi)\rangle$ the related symmetric state of $2j$ qubits. As we shall see, both states have the same *Majorana representation*, $\mathcal{M}(|\psi\rangle) = \mathcal{M}(|F(\psi)\rangle)$.

Interestingly, there is another way of presenting a symmetric state of $2j$ qubits. Consider the collection of $2j$ quantum states

$$|\Phi_k\rangle = \cos(\frac{\theta_k}{2}) |0\rangle + e^{i\phi_k} \sin(\frac{\theta_k}{2}) |1\rangle \quad (9)$$

with $\theta_k \in [0, 2\pi]$, $\phi_k \in [0, \pi]$ and $k = 1, \dots, 2j$. A symmetric superposition of their tensor products constitutes a symmetric state

$$|\psi_{sym}\rangle = \mathcal{N} \sum_{\sigma \in \mathbb{S}_{2j}} |\Phi_{\sigma(1)}\rangle \otimes \dots \otimes |\Phi_{\sigma(2j)}\rangle, \quad (10)$$

where $\sigma \in \mathbb{S}_{2j}$ runs over all permutations of indices, and \mathcal{N} denotes the normalization factor. A connection between those two representations of symmetric

states (7) and (10) is given by the Majorana representation. Consider a symmetric state (7) with state coefficients Z_k . The related Majorana polynomial $w(z)$, Eq. (4), has $2j$ roots z_i with respect to z variable. On one hand, the stereographic projection $z_k \mapsto (\theta_k, \phi_k)$, given by Eq. (2), maps roots of the polynomial $w(z)$ onto the surface of a sphere. On the other hand, however, the set of angles (θ_k, ϕ_k) provides an alternative description of the symmetric state, as a symmetrization (10) of $2j$ qubit states (9) determined by angles (θ_k, ϕ_k) .

III. MEASURES OF COHERENCE

In this section, we introduce the concept of coherence in spin- j system and provide its quantitative description. Furthermore, we extended those concepts to the notion of coherence on an orthonormal basis.

A spin- j coherent state that points in direction \mathbf{n} in \mathbb{R}^3 is a state $|\mathbf{n}\rangle$ for which the polarization vector \mathbf{p} is of length j i.e.

$$\mathbf{p} \equiv \langle \mathbf{n} | \mathbf{J} | \mathbf{n} \rangle = j\mathbf{n}, \quad (11)$$

where $\mathbf{J} = (J_x, J_y, J_z)$ is the spin- j operator, and \hbar is set to unity. In the Majorana representation, a spin- j coherent state is represented by $2j$ degenerated stars on a sphere. Their position is given by \mathbf{n} . A spin state $|\psi\rangle$ is anticoherent, if its polarization vector vanishes, $\mathbf{p} = \mathbf{0}$. One may introduce higher orders of anticoherence, namely a spin state $|\psi\rangle$ is called *t-anticoherent* [26] if $\langle \psi | (\mathbf{n} \cdot \mathbf{J})^k | \psi \rangle$ is independent of \mathbf{n} for $k = 1, \dots, t$.

For a pure symmetric quantum state of $2j$ subsystems $|\psi\rangle \in \mathcal{H}_2^{\otimes 2j}$, we consider a t-partite reduced density operator,

$$\rho_t(\psi) := \text{tr}_{1, \dots, 2j-t} |\psi\rangle \langle \psi|, \quad (12)$$

and analyze its purity,

$$R_t(|\psi\rangle) := \text{tr}(\rho_t(\psi)^2). \quad (13)$$

This quantity can be used to quantify the coherence of the related system of spin- j particle [28]. Recall that the isomorphism (8) identifies a spin- j system with a symmetric state of $2j$ qubits. Thus, Baguette and Martin [31] introduced the following measures of anticoherence of order $t \geq 1$ based on the purity of the reduced state:

$$\mathcal{A}_t(|\psi\rangle) = \frac{t+1}{t} [1 - R_t(F(|\psi\rangle))]. \quad (14)$$

where $|\psi\rangle \in \mathcal{H}_{2j+1}$ is a spin- j system, and $F(|\psi\rangle) \in \mathcal{H}_2^{\otimes 2j}$ denotes the corresponding symmetric state, see the map (8). As discussed in Ref. [31] this quantity enjoys the following properties,

1. $\mathcal{A}_t(|\psi\rangle) = 0 \iff |\psi\rangle$ is coherent,
2. $\mathcal{A}_t(|\psi\rangle) = 1 \iff |\psi\rangle$ is t-anticoherent,
3. $\mathcal{A}_t(|\psi\rangle) \in [0, 1]$ for all $|\psi\rangle$.

4. $\mathcal{A}_t(|\psi\rangle)$ is invariant under phase changes and spin rotations,

and hence provides a plausible measure of *t*-anticoherence. Making use of this quantity we propose the t-coherence measure \mathcal{B}_t for an orthonormal basis using the arithmetic mean of *t*-anticoherence measure of constituting states

$$\mathcal{B}_t(U) = 1 - \sum_{i=1}^N \frac{\mathcal{A}_t(|\psi_i\rangle)}{N}. \quad (15)$$

Here $N=2j+1$ denotes the dimension of the Hilbert space, U is a unitary matrix that represents a basis and $|\psi_i\rangle$ is i-th state in this basis. Observe that the smaller value of the quantity $\mathcal{B}_t(U)$, defined in Eq. (15), the less coherent, hence the more anticoherent, is the analyzed basis determined by the unitary matrix U .

IV. BASES OF EXTREME COHERENCE

In this section, we present the most coherent and the least coherent (the most anticoherent) bases in small dimensions. Note that such bases can be interpreted as orthogonal measurements of extreme coherence. We present both, numerical and analytical results in dimensions $N = 3, 4, 5, 6, 7$, which correspond to spin $j = 1, \frac{3}{2}, 2, \frac{5}{2}, 3$. For convenience, we present the basis vectors $\{|\psi_i\rangle\}$ in the form of a unitary matrix U , where the i-th column of the matrix U corresponds to the i-th vector $|\psi_i\rangle$ in the basis expressed in the angular momentum basis J_z , i.e. $U = (U_{ki})$, where $U_{ki} = \langle j, j+1-k | \psi_i \rangle$. Unitary matrices corresponding to the basis maximizing, respectively minimizing, coherence measure \mathcal{B}_1 in dimension $N = 2j+1$ shall be denoted by U_N^{\max} , U_N^{\min} respectively. In general, basis of extreme coherence correspond to highly symmetric constellations of stars in the Majorana representation, see Fig. (2-10).

Note that the measures of coherence are invariant under $SU(2)$ transformations represented as an action of, Wigner D-matrices. Any such action corresponds to the rotation of a sphere in the Majorana representation, for more details see Appendix E and F.

A Bases for $N=3$

Consider an orthonormal basis in \mathcal{H}_3 , corresponding to $j = 1$. Up to $SU(2)$ transformations, corresponding to the rigid rotation of the entire sphere, any basis can be parametrized by three real parameters, see Appendix A. Coherence measures are invariant under the $SU(2)$ transformations, so one may use this parameterization to find bases of extreme coherence. Therefore, the problem reduces to finding the global extrema of a function of three real variables $\mathcal{B}_1(\Theta_1, \Theta_2, \Phi)$, which we solved analytically. The most coherent basis, for which coherence measure $\mathcal{B}_1 = \frac{8}{9}$,

consists the following states,

$$\begin{aligned} |\psi_3^{max}\rangle &= \frac{1}{\sqrt{3}}(|1,1\rangle + |1,0\rangle + |1,-1\rangle), \\ |\psi'_3^{max}\rangle &= \frac{1}{\sqrt{3}}(|1,1\rangle + \omega_3|1,0\rangle + \omega_3^2|1,-1\rangle), \\ |\psi''_3^{max}\rangle &= \frac{1}{\sqrt{3}}(|1,1\rangle + \omega_3^2|1,0\rangle + \omega_3|1,-1\rangle), \end{aligned} \quad (16)$$

where $\omega_3 = e^{2\pi i/3}$. Basis represented in the Majorana representation is depicted in Fig. 2. Each state in this basis can generate another two states by rotation around \hat{z} axis by angle $2\pi/3$ and $4\pi/3$. All stars lie on the equator. This basis corresponds to the *Fourier* matrix

$$U_3^{max} = F_3 = \frac{1}{\sqrt{3}} \begin{pmatrix} 1 & 1 & 1 \\ 1 & \omega_3 & \omega_3^2 \\ 1 & \omega_3^2 & \omega_3 \end{pmatrix}. \quad (17)$$

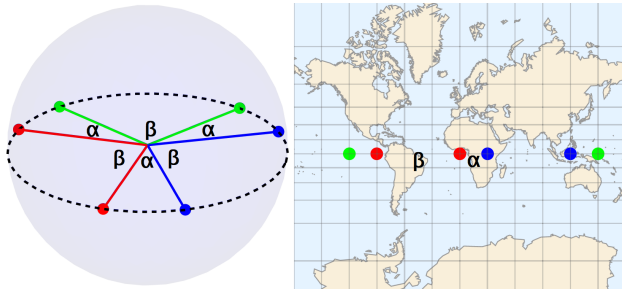


FIG. 2: The most coherent basis (17) in \mathcal{H}_3 ($j = 1$) is represented by three pairs of stars in the Majorana representation. Each state is presented as two dots of given color at the equator. The angles between lines connecting stars with the center of the sphere read $\alpha = \pi/6$ and $\beta = \pi/2$. The left panel shows the stars on the sphere while the right one uses the Mercator projection, with the geographic grid drawn.

The least coherent basis, for which coherence measure $\mathcal{B}_1 = 0$ reads

$$\begin{aligned} |\psi_3^{min}\rangle &= |1,0\rangle, \\ |\psi'_3^{min}\rangle &= \frac{1}{\sqrt{2}}(|1,1\rangle + |1,-1\rangle), \\ |\psi''_3^{min}\rangle &= \frac{1}{\sqrt{2}}(|1,1\rangle - |1,-1\rangle). \end{aligned} \quad (18)$$

This basis corresponds to the following unitary matrix

$$U_3^{min} = \frac{1}{\sqrt{2}} \begin{pmatrix} 0 & 1 & 1 \\ \sqrt{2} & 0 & 0 \\ 0 & 1 & -1 \end{pmatrix}, \quad (19)$$

which is up to a permutation equivalent to the simple sum of a Hadamard matrix H_2 and identity. In the stellar representation, the points representing a single state lie on a line, going through the center of a sphere that graphically corresponds to 1-simplex Δ_1 . The entire constellation spans a regular octahedron, see Fig. 3. This basis may be generated by rotating one of its elements around a vector directed to the

center of any face of a regular octahedron by $2\pi/3$. Observe that the same constellation represents 3 mutually unbiased bases (MUB) in \mathcal{H}_2 i.e. two points of the same color correspond to a single basis.

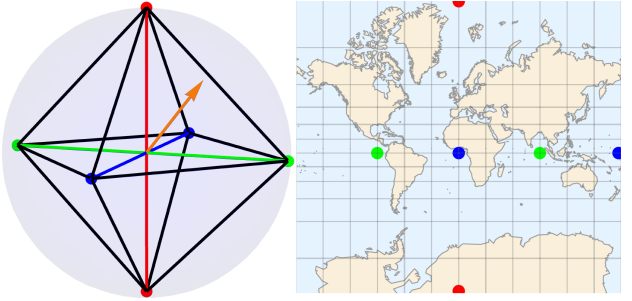


FIG. 3: The least coherent basis (19) in \mathcal{H}_3 ($j = 1$) represented by three pairs of points on the sphere (left). The same configuration in the Mercator projection is shown on the right. The Orange arrow represents one of the rotational axes that may be used to generate the entire basis by rotation of one state by $2\pi/3$ and $4\pi/3$.

Since the most coherent basis in dimension $N = 3$ was found as an analytical solution of maximizing the $\mathcal{B}_1(\Theta_1, \Theta_2, \Phi)$ function, while the least coherent basis saturates the bound for the coherence measure \mathcal{B}_1 , we can summarize this section in the following statement.

Theorem 1. The most coherent and the least coherent bases in \mathcal{H}_3 are presented in Eqs. (16) and (18), and correspond to U_3^{max} and U_3^{min} respectively. The measure of coherence \mathcal{B}_1 archives values $\mathcal{B}_1(U_3^{max}) = \frac{8}{9}$ and $\mathcal{B}_1(U_3^{min}) = 0$.

B Bases for N=4

To find a basis that maximizes average coherence we apply a random walk algorithm. We choose a random unitary matrix U_0 , that represents an orthonormal basis, then we make a random step

$$U_0 \rightarrow U_1 = U_0 \exp(i\alpha H), \quad (20)$$

where α is a small real parameter ("step length") and H is a random hermitian matrix. If $\mathcal{B}_1(U_1) > \mathcal{B}_1(U_0)$, then we treat U_1 as new basis U_0 and repeat the procedure. Otherwise, we pick another random hermitian matrix H and repeat the above steps. During the procedure parameter α is decreased in a way to obtain an extremal basis with an increased precision. Analogously, one can obtain bases that minimize the average coherence using a similar approach.

According to the above algorithm the most coherent basis for $N = 4$ ($j = 3/2$) was found, for which $\mathcal{B}_1 = \frac{8}{9}$, see Fig. 4. This basis is formed by four states which are equivalent up to $SO(3)$ rotation on a sphere. To show that this solution yields a local extremum, one should check that the gradient vanish, $\nabla \mathcal{B}_1(U) = \mathbf{0}$ and the Hessian is negative definite (for maximum) or positive definite (for minimum). For further details see Appendix D. This basis corresponds

to the following unitary matrix

$$U_4^{max} = \frac{1}{3\sqrt{4-2\sqrt{2}}} \begin{pmatrix} \mu & \mu/\sqrt{3} & \mu/\sqrt{3} & 3x^3i \\ \nu & \nu e^{\frac{-2\pi i}{3}} & \nu e^{\frac{2\pi i}{3}} & 0 \\ \zeta & \zeta e^{\frac{2\pi i}{3}} & \zeta e^{\frac{-2\pi i}{3}} & 0 \\ \tau & \tau/\sqrt{3} & \tau/\sqrt{3} & -3i \end{pmatrix}, \quad (21)$$

where $\mu = 3$, $\nu = 3(2 - \sqrt{2})$, $\zeta = 2(3 - \sqrt{2})$, and $\tau = 3(3 - 2\sqrt{2})$. This result was obtained by observation of specific symmetries of purely numerical expression and then using them as constraints to reduce the problem of finding a basis to one real parameter x problem, which helped to get an analytical solution for the local extremum.

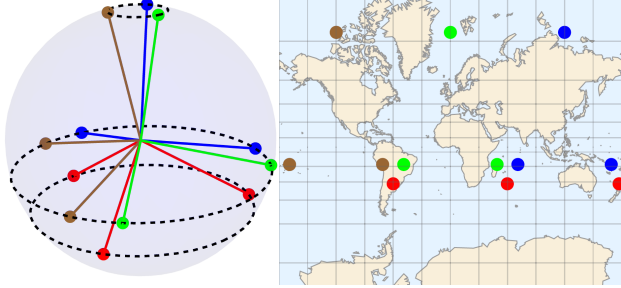


FIG. 4: The most coherent basis (21) in \mathcal{H}_4 ($j = 3/2$) represented by 4 triples of points. The sphere (left) and the Mercator projection (right).

The least coherent basis, see Fig. 5, for which $\mathcal{B}_1 = 0$ corresponds to following unitary matrix

$$U_4^{min} = \frac{1}{\sqrt{6}} \begin{pmatrix} \sqrt{3} & 1 & 1 & 1 \\ 0 & \xi & \xi\omega_3 & \xi\omega_3^2 \\ 0 & \xi & \xi\omega_3^2 & \xi\omega_3 \\ -\sqrt{3} & 1 & 1 & 1 \end{pmatrix}, \quad (22)$$

where $\omega_3 = e^{i2\pi/3}$ and $\theta_3 = \arcsin(1/\sqrt{3})$ with $z_3 = \tan \frac{\theta_3}{2} e^{-i5\pi/6}$ and $\xi = (1 + z_3 + 1/z_3)/\sqrt{3}$.

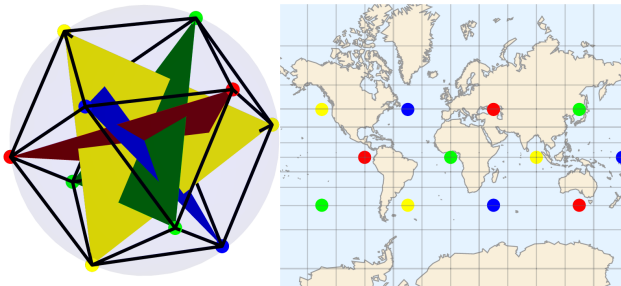


FIG. 5: The least coherent basis in \mathcal{H}_4 ($j = 3/2$) represented by $4 \times 3 = 12$ points. The sphere (left) and the Mercator projection (right). Three stars representing a single state span an equilateral triangle. Constellation of the entire basis spans cuboctahedron, the edges are denoted by black lines.

In analogy to the most coherent basis, the four states are equivalent up to $SO(3)$ rotation on a sphere. The entire basis may be generated by rotating a single state by multiples of $\pi/2$ around the \mathbf{z} axis. Each vector of the basis is represented by three stars that

form an equilateral triangle, then graphically it corresponds to the 2-simplex Δ_2 . The entire constellation of 12 stars forms an Archimedean solid, called cuboctahedron, see Fig. 5.

The least coherent basis U_4^{min} saturates the bound for the measure \mathcal{B}_1 , which leads to the following statement.

Theorem 2. The least coherent basis in \mathcal{H}_4 is U_4^{min} , given by (22) for which $\mathcal{B}_1 = 0$.

Conjecture 1. The most coherent basis in \mathcal{H}_4 is U_4^{max} , given by (21) for which $\mathcal{B}_1 = \frac{8}{9}$.

C Bases for N=5

Using the numerical procedure described above, we found the most coherent basis presented in Fig. 6. The set of states forming this basis can be divided into two equivalence classes, with respect to rotation on the sphere. The first class contains two states

$$|\psi_5^{max}\rangle = \mathcal{N}_1(|2, 2\rangle + \frac{r_1^3}{2} |2, -1\rangle), \quad (23)$$

where $r_1 \in \mathbb{R}$ is the only possible parameter that does not change the symmetry of the state and \mathcal{N}_1 is the normalization constant. The other is obtained by rotation around the \mathbf{x} axis by angle π . The second class contains the state

$$|\psi_5^{max}\rangle = \mathcal{N}_2(|2, 2\rangle + \chi |2, 1\rangle + \sqrt{\frac{2}{3}} |2, 0\rangle + \chi |2, -1\rangle + |2, -2\rangle) \quad (24)$$

and its rotations by angles $2\pi/3$ and $4\pi/3$ around the \mathbf{z} axis. Here, \mathcal{N}_2 is the normalization constant, $\chi = (r_2 + 1/r_2 + 2 \cos \phi_3)/2$, and $r_2, \phi_3 \in \mathbb{R}$ are parameters of symmetry of this class of states.

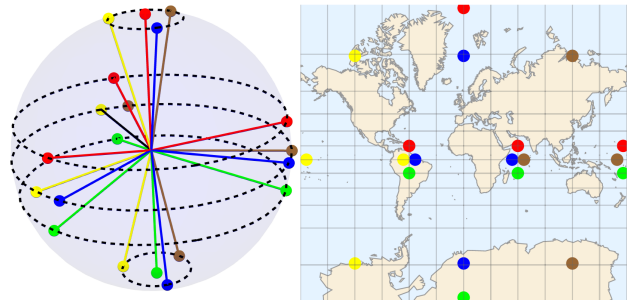


FIG. 6: The most coherent basis in \mathcal{H}_5 ($j = 2$) represented by $5 \times 4 = 20$ points. The sphere (left) and the Mercator projection (right).

In the stellar representation, $|\psi_5^{max}\rangle$ corresponds to one star at the north pole, and another three equally distributed on the circle of latitude, which the horizontal angle θ_4 in spherical coordinates is given by $r_1 = \tan \frac{\theta_4}{2}$, see red stars on Fig. 6. Similarly $|\psi_5^{max}\rangle$ is represented by one star which horizontal angle θ_5 in spherical coordinates is given by $r_2 = \tan \frac{\theta_5}{2}$. Horizontal angle θ_6 of the second star is given by $1/r_2 = \tan \frac{\theta_6}{2}$, so that $\theta_6 = \pi - \theta_5$. The remaining

two stars lie on the equator with azimuthal angles ϕ_3 and $-\phi_3$, see blue stars in Fig. 6.

Imposing those symmetries and orthogonality conditions reduces the number of degrees of freedom to a single one. The maximum of the coherence measure obtained numerically reads, $\mathcal{B}_1 \approx 0.874$ -see Appendix B.

To distinguish the least coherent basis from the others, for which we get $\mathcal{B}_1 = 0$, we impose a condition concerning the second quantity \mathcal{B}_2 . We arrived at the basis for which $\mathcal{B}_2 = \mathcal{B}_1 = 0$. Exactly the same basis was earlier described by Zimba in [26]. It is formed by five states equivalent up to rotation on the sphere. Each of those states is represented by four stars that form a regular tetrahedron, then graphically it corresponds to 3-simplex Δ_3 . It may be constructed by rotation of a state

$$|\psi_5^{tet}\rangle = \frac{1}{\sqrt{3}}(|2,2\rangle + \sqrt{2}|2,-1\rangle). \quad (25)$$

The corresponding unitary matrix reads

$$U_5^{min} = \frac{1}{\sqrt{5}} \begin{pmatrix} 1 & 1 & 1 & 1 & 1 \\ -\kappa & -\kappa\omega_5 & -\kappa\omega_5^2 & -\kappa\omega_5^3 & -\kappa\omega_5^4 \\ \lambda & \lambda\omega_5^2 & \lambda\omega_5^4 & \lambda\omega_5^6 & \lambda\omega_5^3 \\ \kappa & \kappa\omega_5^3 & \kappa\omega_5^6 & \kappa\omega_5^4 & \kappa\omega_5^2 \\ 1 & \omega_5^4 & \omega_5^3 & \omega_5^2 & \omega_5 \end{pmatrix}, \quad (26)$$

where $\kappa = \frac{1}{4}(1 + i\sqrt{15})$, $\lambda = \sqrt{-\kappa}$ and $\omega_5 = e^{i2\pi/5}$. The entire constellation of basis consists of 20 stars and forms a regular dodecahedron, see Fig. 7. Above considerations arrive to the following statement.

Theorem 3. The least coherent basis in \mathcal{H}_5 is U_5^{min} , for which $\mathcal{B}_1 = \mathcal{B}_2 = 0$.

Conjecture 2. The most coherent basis in \mathcal{H}_5 is U_5^{max} , for which $\mathcal{B}_1 \approx 0.874$.

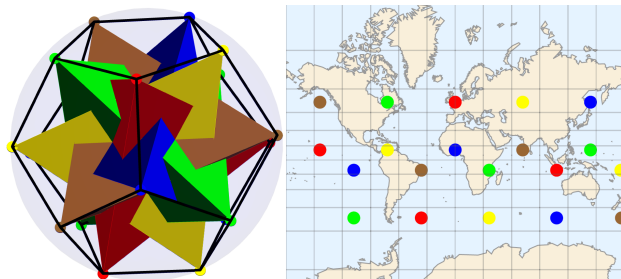


FIG. 7: The least coherent basis (26) in \mathcal{H}_5 ($j = 2$) represented by $5 \times 4 = 20$ points on the sphere (left) and in the Mercator projection (right). Stars representing each state span a regular tetrahedron and the entire basis forms a compound of five tetrahedra and spans a regular dodecahedron, plotted with solid lines.

Note that a regular dodecahedron arises in quantum theory in several contexts, including the Penrose dodecahedron [50–52] formed by 40 pure states in \mathcal{H}_4 which allow one to construct a proof of the Bell’s non-locality theorem. The same configuration is related to the set of five isoentangled two-qubit mutually unbiased bases, are the partial traces of 20 pure states in \mathcal{H}_4 lead to a regular dodecahedron inside the Bloch ball [53].

D Bases for N=6

The most coherent basis found by the numerical search has an octahedral symmetry, see Fig. 8. All states in this basis are equivalent up to a rotation. By imposing this symmetry and orthogonality requirement one gets an analytical expression for that basis, for which $\mathcal{B}_1(U_6^{max}) = (929 + 272\sqrt{10})/2025 \approx 0.874$. The basis contains the state,

$$|\psi_6^{max}\rangle = \mathcal{N}_3 \left(\left| \frac{5}{2}, \frac{5}{2} \right\rangle - \frac{1}{3}(2\sqrt{2} - \sqrt{5}) \left| \frac{5}{2}, -\frac{3}{2} \right\rangle \right) \quad (27)$$

and the remaining five states, which may be obtained by appropriate rotations, where \mathcal{N}_3 denotes the normalization constant. In the Majorana representation, a state $|\psi_6^{max}\rangle$ is represented by a single star at the north pole and the remaining four equally distributed on a parallel with latitude defined by $\tan \frac{\theta_7}{2} = (\frac{1}{3}(2\sqrt{10} - 5))^{1/4}$, see red stars in Fig. 8. The corresponding unitary matrix reads

$$U_6^{max} = \frac{1}{2} \begin{pmatrix} 2a & 0 & -b & -b & -b & -b \\ 0 & 2b & a & -a & -ia & ia \\ 0 & 0 & 1 & 1 & -1 & -1 \\ 0 & 0 & 1 & -1 & i & -i \\ 2b & 0 & a & a & a & a \\ 0 & 2a & -b & b & ib & -ib \end{pmatrix}, \quad (28)$$

where $a = \frac{1}{3}\sqrt{11/2 + \sqrt{10}}$ and $b = (2 - \sqrt{10})/6$.

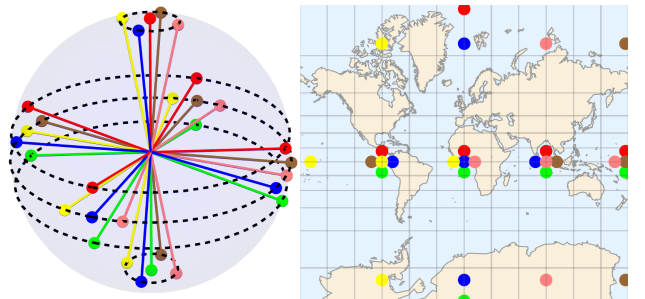


FIG. 8: The most coherent basis in \mathcal{H}_6 ($j = 5/2$) represented by $6 \times 5 = 30$ points. The sphere (left) and the Mercator projection (right).

In a manner reminiscent of the $N = 5$ case, we employ further conditions to identify a unique least coherent basis. Specifically, we require that not only that \mathcal{B}_1 is minimal, but \mathcal{B}_2 is also optimal. We find a basis for which $\mathcal{B}_1 = 0$ and $\mathcal{B}_2 \approx 0.092$, without expected symmetries. However, when we impose the minimization of a sum of measures \mathcal{B}_1 and \mathcal{B}_2 , we obtained $\mathcal{B}_1, \mathcal{B}_2 > 0$ and observe the emergence of an intriguingly symmetric structure. This basis is comprised of 30 points that are equally distributed across five circles of latitude on a sphere, with each circle hosting six stars in vertices of a regular hexagon. The Majorana representation of this basis is displayed in Fig. 9. A single state is represented, up to rotation, by a set of points in spherical coordinates (θ, ϕ) given

by

$$\{(\pi/2, 0), (\theta_8, 5\pi/6 - \delta_1), (\theta_9, -\pi/2 - \delta_2), (\pi - \theta_8, -5\pi/6 + \delta_1), (\pi - \theta_9, \pi/2 + \delta_2)\}. \quad (29)$$

The remaining four states can be obtained through rotation around the \hat{z} axis by an angle of $\pi/3$. Based on numerical experiments, we have imposed this parametrization and obtained numerical results for the four real parameters $\theta_8, \theta_9, \delta_1$, and δ_2 , resulting in one state described by Eq. (29) and four rotations. These rotations generate mutually orthogonal states up to the accuracy of approximately 10^{-8} . This particular basis, which we denote as \hat{U}_6^{min} , yields $\mathcal{B}_1 \approx 0.000006$ and $\mathcal{B}_2 \approx 0.010709$. It minimizes a measure that is a sum of \mathcal{B}_1 and \mathcal{B}_2 , also it has interesting rotational symmetries. See Appendix B for further details of numerical results.

Conjecture 3. The most coherent basis in \mathcal{H}_6 is U_6^{max} for which $\mathcal{B}_1 = \frac{929-272\sqrt{10}}{2025} \approx 0.884$, see Eq. (28).

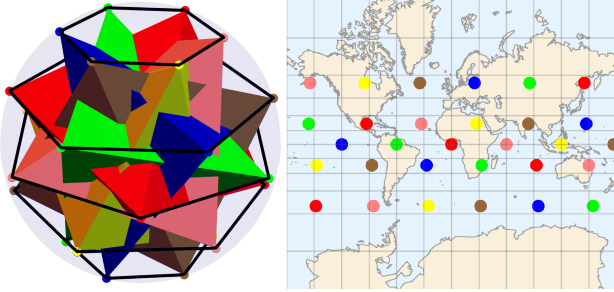


FIG. 9: The selected least coherent basis in \mathcal{H}_6 ($j = 5/2$), for which the sum of \mathcal{B}_1 and \mathcal{B}_2 achieves minimum. It is represented by $6 \times 5 = 30$ points. The sphere with a regular hexagon on each circle of latitude (left) and the Mercator projection (right).

E Basis for N=7

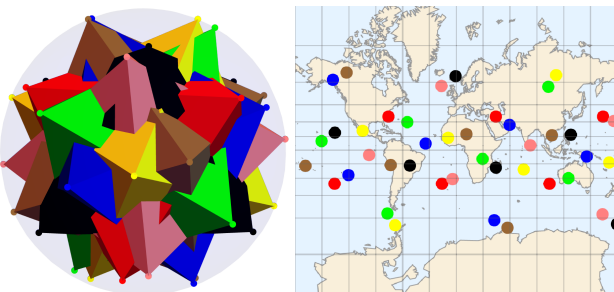


FIG. 10: The least coherent basis in \mathcal{H}_7 ($j = 3$) represented by $7 \times 6 = 42$ points. Each state is represented by a regular octahedron. The sphere (left) and the Mercator projection (right).

The least coherent basis U_7^{min} , found by numerical search is formed by seven regular octahedrons, see

Fig. 10. All states in this basis are equivalent up to rotation to the state

$$|\psi_7^{oct}\rangle = \frac{1}{\sqrt{2}}(|3, -2\rangle + |3, 2\rangle). \quad (30)$$

No symmetry has been observed in the relative positions of those octahedrons. Additional details regarding the numerical results can be found in Appendix B.

Theorem 4. The least coherent basis in \mathcal{H}_7 is represented by U_7^{min} for which $\mathcal{B}_1 = \mathcal{B}_2 = \mathcal{B}_3 = 0$ and $\mathcal{B}_4 = \frac{1}{6}$.

F Asymptotic results

We observed that the average value of the introduced t-coherence measure $\mathcal{B}_t(U)$ decreases with the dimension N of the Hilbert space \mathcal{H}_N for any t , see Fig. 11 as an example. One can demonstrate that the value of $\mathcal{B}_t(U)$, averaged over the unitary group with respect to the Haar measure, approaches zero as the dimension N tends to infinity.

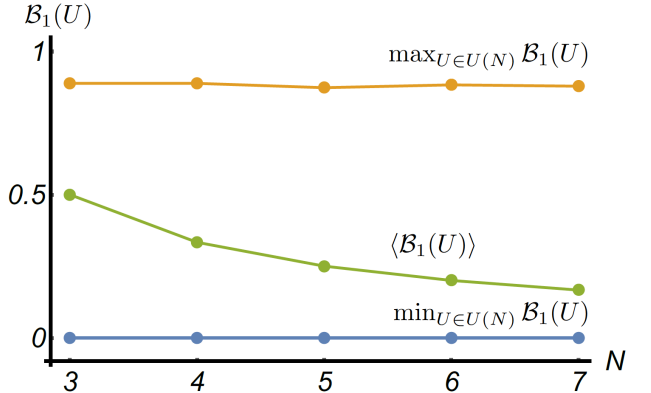


FIG. 11: Maximal, minimal and average value of the coherence measure \mathcal{B}_1 as a function of the dimension $N = 2j + 1$. The average values are taken with respect to the Haar measure on $U(N)$. The solid line is plotted to guide the eye.

V. PERMUTATION SYMMETRIC STATES OF MULTIQUBIT SYSTEMS

Due to the correspondence (8) between spin- j states and symmetric states of $2j$ spin-1/2 particles and the fact that our measure of 1-anticoherence Eq. (14) is equivalent to linear entropy of reduced density operator, the extremal bases we found correspond to the most and the least entangled bases. Specifically, the 1-anticoherent states $\mathcal{A}_1(|\psi\rangle) = 1$ are maximally entangled, while the coherent states $\mathcal{A}_1(|\psi\rangle) = 0$ represent separable states of the composite system.

Note that the basis (19), represented in Fig. 3 by a regular octahedron, is equivalent to the well-known

Bell basis in the symmetric sector of $\mathcal{H}_2^{\otimes 2}$,

$$\begin{aligned} |\psi_1\rangle &= \frac{1}{\sqrt{2}}(|01\rangle + |10\rangle), \\ |\psi_2\rangle &= \frac{1}{\sqrt{2}}(|00\rangle + |11\rangle), \\ |\psi_3\rangle &= \frac{1}{\sqrt{2}}(|00\rangle - |11\rangle). \end{aligned} \quad (31)$$

The last state that completes the orthonormal basis of $\mathcal{H}_2^{\otimes 2}$ is a singlet state

$$|\psi_4\rangle = \frac{1}{\sqrt{2}}(|01\rangle - |10\rangle), \quad (32)$$

which does not belong to the symmetric subspace. Similarly, the least coherent basis in \mathcal{H}_4 corresponds to a basis of the symmetric subspace of $\mathcal{H}_2^{\otimes 3}$, that is maximally entangled, and each state is equivalent (up to $SU(2)$ rotation) to a *GHZ* state [4]

$$|GHZ\rangle = \frac{1}{\sqrt{2}}(|000\rangle + |111\rangle). \quad (33)$$

In \mathcal{H}_5 , the least coherent basis (26), represented in Fig. 7 by five regular tetrahedrons that form a regular dodecahedron, corresponds to a basis of symmetric sector of $\mathcal{H}_2^{\otimes 4}$. This basis consists five, maximally entangled states of four qubits, which are known to be the most sensitive states for alignment of the reference frame [20] and having the highest geometric entanglement [13]. A simple calculation leads to the form

$$\begin{aligned} |\psi_{tet.}\rangle &= \frac{1}{\sqrt{3}}|0000\rangle + \frac{1}{\sqrt{6}}(|0111\rangle \\ &\quad + |1011\rangle + |1101\rangle + |1110\rangle). \end{aligned} \quad (34)$$

In a similar way the matrix U_7^{min} of minimal coherence leads to the basis of the symmetric sector of $\mathcal{H}_2^{\otimes 6}$ with the maximal entanglement. Each state is equivalent, up to rotation, to

$$|\psi_{oct.}\rangle = \frac{1}{\sqrt{2}}(|D_{6,1}\rangle - |D_{6,5}\rangle), \quad (35)$$

which is known to display the highest geometric entanglement [13].

VI. CONCLUDING REMARKS

This study introduces measures of t -coherence \mathcal{B}_t as tools to characterize the spin coherence of a given basis in \mathcal{H}_N . The search for the least coherent bases

for $N = 3, 4, 5$ and 7 is performed, and a set of candidates for the most coherent bases for $N = 3, 4, 5, 6$ is presented. Some of these bases analyzed by Majorana representation reveal symmetries of Platonic solids. Obtained results, including the most coherent, anticoherent, and average values of \mathcal{B}_1 , are presented in Fig. 11 and summarized in Table I. These bases lead to orthogonal measurements of Lüders and von Neumann of extreme spin coherence.

Coherent and anticoherent states have practical applications in quantum metrology as optimal rotosensors [32–35]. This work provides a natural extension of previous studies on the search for such states proposing optimal measurements. Note that presented bases have specific rotational symmetries, which allow one to obtain the entire basis just by rotation of a reference state and therefore make it easier to prepare.

N	\mathcal{B}_1	Anticoherent			
		\mathcal{B}_1	\mathcal{B}_2	\mathcal{B}_3	\mathcal{B}_4
3	$8/9 \approx 0.889$	0	-	-	-
4	$8/9 \approx 0.889$	0	$1/4$	-	-
5	0.874	0	0	$1/3$	-
6	$\frac{929+272\sqrt{10}}{2025} \approx 0.874$	0.000006	0.011	0.110	0.375
7	-	0	0.091	0.192	0.375
		0	0	0	$1/6$

TABLE I: Measures of t -coherence for identified bases of order $N = 3, \dots, 7$. Analytical results are shown in bold purple, while analytical results with constraints suggested by numerical outcomes are shown in blue. The remaining bases were obtained via numerical search with imposed symmetry constraints to enhance precision.

VII. ACKNOWLEDGEMENTS

We would like to express our gratitude to Rafał Bistroń and Jakub Czartowski for engaging in discussions that have enriched this research significantly. We are also thankful to the Foundation for Polish Science for the financial support provided through TEAM-NET project number POIR.04.04.00-00-17C1/18-00 and to the Narodowe Centrum Nauki for the support provided through the Quantera project number 2021/03/Y/ST2/00193. A. B. acknowledges support by an NWO Vidi grant (Project No. VI.Vidi.192.109).

APPENDIX A: PARAMETRIZATION OF BASES IN \mathcal{H}_3

Any basis in \mathcal{H}_3 , up to a $SU(2)$ rotation, consisting of states $|\Psi_3\rangle$, $|\Psi'_3\rangle$ and $|\Psi''_3\rangle$ can be expressed in terms of three real parameters Θ_1, Θ_2, Φ . A parameterization of orthonormal bases is given by

$$\begin{aligned} |\Psi_3\rangle &= \mathcal{N}_4(|1,1\rangle - \tan^2 \frac{\Theta_1}{2} |1,-1\rangle), \\ |\Psi'_3\rangle &= \mathcal{N}_5(|1,1\rangle + \Upsilon |1,0\rangle + \cot^2 \frac{\Theta_1}{2} |1,-1\rangle), \\ |\Psi''_3\rangle &= \mathcal{N}_6(|1,1\rangle - \frac{1 + \cot^4 \frac{\Theta_1}{2}}{\Upsilon^*} |1,0\rangle + \cot^2 \frac{\Theta_1}{2} |1,-1\rangle), \end{aligned} \quad (36)$$

where $\mathcal{N}_4, \mathcal{N}_5, \mathcal{N}_6$ denote suitable normalization constants, and $\Upsilon = (e^{-i\Phi} \cot \frac{\Theta_2}{2} \cot^2 \frac{\Theta_1}{2} + e^{i\Phi} \tan \frac{\Theta_2}{2})/\sqrt{2}$. In the Majorana representation, the state $|\Psi_3\rangle$ is represented by two points on the opposite sites of a single circle of latitude, given by angle Θ_1 in the spherical coordinates.

APPENDIX B: NUMERICAL RESULTS

In this section we present some details concerning our numerical results. Detailed expressions for the vectors forming orthonormal bases found numerically are available online [55].

N = 5

The most coherent basis in \mathcal{H}_5 , for which $\mathcal{B}_1 \approx 0.8736987$ is generated by rotation of two reference states (23) and (24) with parameters $\chi = (r_2 + 1/r_2 + 2 \cos \phi)/2$ and $r_1 = \sqrt[3]{4/(1/r_2^2 + r_2^2 + 2 \cos \phi)}$. Numerical search gives the following values of free parameters $r_2 \approx 7.564405$ and $\phi \approx 0.93380835$. The basis is orthonormal up to accuracy $\sum_{i,j,k} |U_{ij}^* U_{ik} - \delta_{jk}| \approx 2.1 \times 10^{-15}$.

N = 6

Minimizing \mathcal{B}_1 leads to several different bases with $\mathcal{B}_1 \approx 0$, without any internal symmetry. To distinguish among them we analyzed a linear combination of \mathcal{B}_1 and \mathcal{B}_2 . The measure \mathcal{B}_1 is no longer ≈ 0 , but interesting rotational symmetry by $\pi/3$ and internal state symmetry (29) arise. Imposing such symmetries we search for orthonormal basis generated by rotating state $|\psi_6^{min}\rangle$ of internal symmetry (29) around the \hat{z} axis by $\pi/3$. The numerical search gave us the following values of the parameters $\theta_8 \approx 0.5922575$, $\theta_9 \approx 1.1820735$, $\delta_1 \approx 0.0822441$, $\delta_2 \approx 0.0522207$. Corresponding reference vector in \mathcal{H}_6 reads,

$$|\psi_6^{min}\rangle \approx (0.4082482, -0.3757166 - 0.1596989i, 0.0850774 - 0.3992850i, 0.0850774 - 0.3992850i, -0.3757166 - 0.1596989i, 0.4082483).$$

The other four vectors are obtained by rotation of $|\psi_6^{min}\rangle$ around the \hat{z} axis by an angle of $\pi/3$. Rotation matrix reads $\hat{R}_{\hat{z}}(\pi/3) = \text{diag}(1, e^{i\pi/3}, e^{i2\pi/3}, e^{i\pi}, e^{i4\pi/3}, e^{i5\pi/3})$ and the entire basis takes the form

$$\{\hat{R}_{\hat{z}}(\pi/3)^k |\psi_6^{min}\rangle\}_{k=0}^5.$$

Obtained constellation of vectors provides the following values of the measures $\mathcal{B}_1 \approx 0.0000059$, $\mathcal{B}_2 \approx 0.0107090$ and $\mathcal{B}_3 \approx 0.1206302$. The basis is orthonormal up to accuracy $\sum_{i,j,k} |U_{ij}^* U_{ik} - \delta_{jk}| \approx 9.4 \times 10^{-7}$.

N = 7

The basis U_7^{min} is orthonormal with accuracy $\sum_{i,j,k} |U_{ij}^* U_{ik} - \delta_{jk}| \approx 6.3 \times 10^{-15}$. Positions of stars representing states in this basis differ from those of regular octahedrons by less than 10^{-15} , for a unit radius of a sphere.

APPENDIX C: COHERENCE MEASURE IN TERMS OF MATRIX ELEMENTS.

The t-anticoherence measure $\mathcal{A}_t(|\psi_i\rangle)$ of a state $|\psi_i\rangle$ is defined in Eq. (14) using purity of corresponding reduced symmetric state $F(|\psi_i\rangle)$, which is discussed in [28, 31]. Thus, the t-coherence measure $\mathcal{B}_t(U)$ of an

orthonormal basis $U = \{|\psi_1\rangle, \dots, |\psi_N\rangle\}$, can be expressed in terms of the purity of a corresponding reduced symmetric states $F(|\psi_i\rangle)$. The purity of a state $F(|\psi_i\rangle)$, corresponding to a state $|\psi_i\rangle$, expressed in angular momentum J_z basis (3) is given by,

$$R_t(|\psi_i\rangle) = \sum_{k_1=0}^t \sum_{k_2=0}^t \left| \sum_{k=-j}^{j-t} Z_{j-k-k_1}^* Z_{j-k-k_2} \Gamma_{j+k}^{k_1 k_2} \right|^2, \quad (37)$$

where

$$\Gamma_k^{k_1 k_2} = \frac{1}{C_t^{2j}} \sqrt{C_k^{k+k_1} C_{t-k_1}^{2j-k-k_1} C_k^{k+k_2} C_{t-k_2}^{2j-k-k_2}} \quad (38)$$

and $C_q^l = \binom{l}{q}$ if $0 \leq l \leq q$ and 0 otherwise. Then the t-coherence measure $\mathcal{B}_t(U)$ of an orthonormal basis, represented by unitary matrix U can be expressed in terms of its matrix elements $U_{ki} = \langle j, j+1-k | \psi_i \rangle$ as follows

$$\mathcal{B}_t(U) = 1 - \frac{t+1}{Nt} \sum_{p=1}^N \left(1 - \sum_{k_1, k_2=0}^t \left| \sum_{k=-j}^{j-t} U_{j-k-k_1+1, p}^* U_{j-k-k_2+1, p} \Gamma_{p+k}^{k_1 k_2} \right|^2 \right). \quad (39)$$

APPENDIX D: EXTREMALITY OF SOLUTION.

Extremal point \mathbf{x}_0 of n-variable function f satisfies $\nabla f|_{\mathbf{x}_0} = \mathbf{0}$. The most convenient way to determine whether it is a local minimum, maximum, or saddle point is the analysis of the positive definiteness of Hessian H_f defined as

$$H_f = \begin{pmatrix} \frac{\partial^2 f}{\partial x_1^2} & \frac{\partial^2 f}{\partial x_1 \partial x_2} & \cdots & \frac{\partial^2 f}{\partial x_1 \partial x_n} \\ \vdots & \vdots & \ddots & \vdots \\ \frac{\partial^2 f}{\partial x_n \partial x_1} & \frac{\partial^2 f}{\partial x_n \partial x_2} & \cdots & \frac{\partial^2 f}{\partial x_n^2} \end{pmatrix}. \quad (40)$$

1. If $H_f|_{\mathbf{x}=\mathbf{x}_0} > 0 \iff \mathbf{x}_0$ is a local maximum.
2. If $H_f|_{\mathbf{x}=\mathbf{x}_0} < 0 \iff \mathbf{x}_0$ is a local minimum.
3. If $H_f|_{\mathbf{x}=\mathbf{x}_0} = 0 \iff \mathbf{x}_0$ is a saddle point.

Following [49] we recall the Lie group structure of unitary matrices manifold to introduce directions in the neighborhood of matrix U . Lie algebra of unitary matrices is formed by Hermitian matrices. We set the following basis

$$\begin{aligned} H_{ii} &= |i\rangle \langle i| \quad \text{for } i \in 1, \dots, N, \\ H_{kl}^+ &= |k\rangle \langle l| + |l\rangle \langle k| \quad \text{for } k, l \in 1, \dots, N, \quad k \neq l, \\ H_{kl}^- &= i(|k\rangle \langle l| - |l\rangle \langle k|) \quad \text{for } k, l \in 1, \dots, N, \quad k \neq l, \end{aligned} \quad (41)$$

that give N^2 directions in neighbourhood of matrix U . Now we may define the derivative of a function f on a unitary matrix as

$$\nabla_r f(U) = \lim_{\epsilon_r \rightarrow 0} \frac{f(U_{\epsilon_r}) - f(U)}{\epsilon_r}, \quad (42)$$

where U_{ϵ_r} is the matrix U , transformed in r -th direction as $U_{\epsilon_r} = U \exp(i\epsilon_r H^r) = U(\mathbb{1} + i\epsilon_r H_r + O(\epsilon_r^2))$, where H^r is an element of the Lie algebra (41).

For a given unitary matrix U the derivative of the coherence measure $\mathcal{B}_t(U)$, determined by Eqs. (15) and (39) reads,

$$\begin{aligned} \nabla_r \mathcal{B}_t(U) = -4 \frac{t+1}{Nt} \sum_{p, p'=1}^N \sum_{k_1, k_2=0}^t \sum_{k, k'=-j}^{j-t} \Gamma_{j+k}^{k_1 k_2} \Gamma_{j+k'}^{k_1 k_2} \text{Im} \left(U_{j-k'-k_1+1, p} U_{j-k'-k_2+1, p}^* \times \right. \\ \left. (U_{j-k-k_1+1, p}^* U_{j-k-k_2+1, p'} H_{p', p}^{r*} - U_{j-k-k_2+1, p} U_{j-k-k_1+1, p'}^* H_{p', p}^{r*}) \right). \end{aligned} \quad (43)$$

In a similar way, we arrive at the second derivative:

$$\begin{aligned} \nabla_r \nabla_s \mathcal{B}_t(U) = -8 \frac{t+1}{Nt} \sum_{p,p',p''=1}^N \sum_{k_1,k_2=0}^t \sum_{k,k'=-j}^{j-t} \Gamma_{j+k}^{k_1 k_2} \Gamma_{j+k'}^{k_1 k_2} \operatorname{Re} \left(U_{j-k'-k_1+1,p} U_{j-k-k_2+1,p} U_{j-k'-k_2+1,p'}^* \times \right. \\ \left. H_{p',p}^{r*} U_{j-k-k_1+1,p''}^* H_{p'',p}^{s*} - U_{j-k'-k_1+1,p} U_{j-k-k_1+1,p}^* U_{j-k'-k_2+1,p}^* H_{p',p}^{r*} U_{j-k-k_2+1,p''} \times \right. \\ \left. H_{p'',p}^s - U_{j-k'-k_1+1,p} U_{j-k'-k_2+1,p}^* U_{j-k-k_1+1,p'}^* H_{p',p}^{r*} U_{j-k-k_2+1,p''} H_{p'',p}^s \right). \end{aligned} \quad (44)$$

APPENDIX E: WIGNER D-MATRICES

Let J_x, J_y, J_z be components of the *angular momentum operator*. The three operators satisfy the following commutation relations

$$[J_x, J_y] = iJ_z \quad [J_z, J_x] = iJ_y \quad [J_y, J_z] = iJ_x, \quad (45)$$

where the reduced Planck's constant is set to identity, $\hbar = 1$. Mathematically, the operators J_x, J_y, J_z generate the Lie algebra $\text{SU}(2)$ and $\text{SO}(3)$. The sum of squares of J_x, J_y, J_z is known as *the Casimir operator*,

$$\mathbf{J}^2 = J_x^2 + J_y^2 + J_z^2 \quad (46)$$

and it commutes with J_x, J_y, J_z operators. In particular, \mathbf{J}^2 might be diagonalized together with J_z , which defines an orthonormal basis of joint eigenvectors labeled by quantum numbers j, m ,

$$\begin{aligned} \mathbf{J}^2 |j, m\rangle &= j(j+1) |j, m\rangle, \\ J_z |j, m\rangle &= m |j, m\rangle, \end{aligned}$$

with $j = 0, \frac{1}{2}, 1, \dots$ and $m = -j, -j+1, \dots, j$. Note that for a given j , the operator J_z is non-degenerated and has exactly $2j+1$ distinct eigenvalues.

A three-dimensional *rotation operator* has the form

$$\mathcal{R}(\alpha, \beta, \gamma) = e^{-i(\alpha J_z + \beta J_y + \gamma J_x)}. \quad (47)$$

The *Wigner D-matrix* [54] is a unitary matrix of dimension $2j+1$ defined in the angular momentum basis as

$$D_{mm'}^j(\alpha, \beta, \gamma) := \langle j, m' | \mathcal{R}(\alpha, \beta, \gamma) | j, m \rangle. \quad (48)$$

Recall, those matrix elements of the operator J_z in the angular momentum basis read

$$\langle j, m' | J_y | j, m \rangle = \frac{1}{2i} \left[\delta_{m',m+1} \sqrt{(j-m)(j+m+1)} - \delta_{m',m-1} \sqrt{(j-m)(j-m+1)} \right], \quad (49)$$

then, the precise form of the Wigner D-matrix for $j = \frac{1}{2}$ is

$$D^{\frac{1}{2}}(\alpha, \beta, \gamma) = \begin{pmatrix} \cos \frac{\beta}{2} e^{-\frac{i}{2}(\alpha+\gamma)} & -\sin \frac{\beta}{2} e^{-\frac{i}{2}(\alpha-\gamma)} \\ \sin \frac{\beta}{2} e^{\frac{i}{2}(\alpha-\gamma)} & \cos \frac{\beta}{2} e^{\frac{i}{2}(\alpha+\gamma)} \end{pmatrix} \quad (50)$$

and for $j = 1$:

$$D^1(\alpha, \beta, \gamma) = \begin{pmatrix} \cos^2 \frac{\beta}{2} e^{-i(\alpha+\gamma)} & -\sqrt{2} \cos \frac{\beta}{2} \sin \frac{\beta}{2} e^{-i\alpha} & \sin^2 \frac{\beta}{2} e^{-i(\alpha-\gamma)} \\ \sqrt{2} \cos \frac{\beta}{2} \sin \frac{\beta}{2} e^{-i\gamma} & \cos \beta & -\sqrt{2} \cos \frac{\beta}{2} \sin \frac{\beta}{2} e^{i\gamma} \\ \sin^2 \frac{\beta}{2} e^{i(\alpha-\gamma)} & \sqrt{2} \cos \frac{\beta}{2} \sin \frac{\beta}{2} e^{i\alpha} & \cos^2 \frac{\beta}{2} e^{-i(\alpha+\gamma)} \end{pmatrix}. \quad (51)$$

APPENDIX F: INVARIANCE UNDER ROTATION

The Majorana representation presents a spin- j state as a collection of $2j$ stars on a sphere. In this section, we discuss the behavior of such a representation, while rotating the sphere. Firstly, we show that the rotation of a sphere preserves the scalar products of related states, in particular, transforming any orthonormal basis into another orthonormal basis. Secondly, we show that the rotation of a sphere preserves the coherence (14) of related states. Lastly, we present the rotation of a sphere in terms of the transformation of related spin- j and symmetric states. As a consequence, all orthonormal bases of extreme spin coherence specified in this work

are defined up to the global rotation of related Majorna stars, or equivalently, up to the action of any Wigner D-matrix on related spin- j basis elements.

Recall that there is a direct correspondence between a unitary evolution of a two-level system and rotations of the related Bloch sphere representation, which follows directly from the fact that groups $SU(2)$ and $SO(3)$ are isomorphic. In particular, any two-dimensional unitary matrix is of the form $U = \begin{pmatrix} a & b \\ -b^* & a^* \end{pmatrix}$, $|a|^2 + |b|^2 = 1$ and hence can be expressed as

$$U(\alpha, \beta, \gamma) = \begin{pmatrix} \cos \frac{\beta}{2} e^{-\frac{i}{2}(\alpha+\gamma)} & -\sin \frac{\beta}{2} e^{-\frac{i}{2}(\alpha-\gamma)} \\ \sin \frac{\theta}{2} e^{\frac{i}{2}(\alpha-\gamma)} & \cos \frac{\theta}{2} e^{\frac{i}{2}(\alpha+\gamma)} \end{pmatrix}. \quad (52)$$

As a quantum state $|\psi\rangle \in \mathcal{H}_2$ can be presented as a single point on the Bloch sphere, its evolution under the above unitary operator might be presented as a sequence of three Euler rotations acting on the Bloch sphere. More precisely, rotation $\mathcal{R}_Z(\alpha)$ of α angle along Z axis, then $\mathcal{R}_X(\beta)$ by β angle along X axis and $\mathcal{R}_Z(\gamma)$ by γ angle along Z axis again on the Bloch sphere. We shall denote such a rotation by $\mathcal{R}(\alpha, \beta, \gamma)$.

Any symmetric state $|\psi\rangle \in \mathcal{H}_2^{\otimes 2j}$ remains symmetric under any action of the joint unitary local operator $U^{\otimes 2j}$ [16]. In fact, the reverse statement is also true, all local unitary operations that preserve a given symmetric state are of the form $U^{\otimes 2j}$ [12]. For a unitary matrix represented in the form (52) the action of $U^{\otimes 2j}$ is equivalent to the rotation $\mathcal{R}(\alpha, \beta, \gamma)$ of the sphere. As a consequence, any rotation of stars in the Bloch representation does not change the scalar product of underlying symmetric states $|\psi_{1,2}\rangle \in \mathcal{H}_2^{\otimes 2j}$ as $\langle \psi_1 | (U^{\otimes 2j})^\dagger U^{\otimes 2j} | \psi_2 \rangle = \langle \psi_1 | \psi_2 \rangle$. In particular, the orthonormal basis is mapped to another orthonormal basis of symmetric states. Furthermore, the purity of the reduced density operator (13) does not change under local unitary transformation $U^{\otimes 2j}$, and hence is the same for states related by the rotation of a sphere in the Majorana representation.

Recall that the system of symmetric states of $2j$ qubits is related to the spin- j system by isomorphism F , see Eq. (8), hence it preserves a scalar product, i.e. $\langle \psi_3 | \psi_4 \rangle = \langle F(\psi_3) | F(\psi_4) \rangle$, where $|\psi_{3,4}\rangle \in \mathcal{H}_{2j+1}$. Furthermore, by the definition, both states $|\psi\rangle$ and $|F(\psi)\rangle$ have the same Majorana representation. As a consequence, any rotation of stars in the Bloch representation of the spin- j system does not change the scalar product of underlying states, as was the case of symmetric states. Moreover, notice that the rotation of a sphere does not change the coherence properties of the represented states. Indeed, for any symmetric state $|F(\psi)\rangle$ the purity of the reduced density operator (13) does not change under local unitary transformation $U^{\otimes 2j}$, or rotation of a sphere in the Majorana representation respectively. Hence, both states initial and rotated achieve the same t -anticoherence (14). We can summarize this discussion in the following two observations.

Observation 1. An action of a joint local unitary operator $U(\alpha, \beta, \gamma)^{\otimes 2j}$ on a collection of symmetric states $\{|\psi_{sym}^k\rangle\}_{k=1}^m$ belonging to $\mathcal{H}_2^{\otimes 2j}$ preserves their mutual scalar products and purity. Furthermore, it is represented by the rotation $\mathcal{R}(\alpha, \beta, \gamma)$ in the stellar representation, i.e.

$$\mathcal{M}\left(U(\alpha, \beta, \gamma)^{\otimes 2j} |\psi_{sym}^k\rangle\right) = \mathcal{R}(\alpha, \beta, \gamma) \mathcal{M}(|\psi_{sym}^k\rangle). \quad (53)$$

Observation 2. An action of a Wigner D-matrix $D^j(\alpha, \beta, \gamma)$ on a collection of spin- j sets $\{|\psi_k\rangle\}_{k=1}^m$ belonging to \mathcal{H}_{2j+1} preserves their mutual scalar products and t -anticoherence measure $\mathcal{A}_t(|\psi_k\rangle)$. Furthermore, it is represented by the rotation $\mathcal{R}(\alpha, \beta, \gamma)$ in the stellar representation, i.e.

$$\mathcal{M}\left(D^j(\alpha, \beta, \gamma) |\psi_k\rangle\right) = \mathcal{R}(\alpha, \beta, \gamma) \mathcal{M}(|\psi_k\rangle). \quad (54)$$

[1] T. Frankel, The Geometry of Physics: An Introduction, 3rd ed., *Cambridge University Press* (2011)

[2] D. Chruściński, and A. Jamiołkowski, Geometric Phases in Classical and Quantum Mechanics, *Birkhäuser* (2004).

[3] D.A. Lee, Geometric relativity, *American Mathematical Society*, Providence (2021).

[4] I. Bengtsson, and K. Życzkowski, Geometry of Quantum States: An Introduction to Quantum Entanglement, 2nd ed., *Cambridge University Press* (2017).

[5] M. Lewin, Geometric methods for nonlinear many-body quantum systems, *J. Functional Analysis* **260**, 12, (2011).

[6] E. Cohen, H. Larocque, F. Bouchard et al., Geometric phase from Aharonov–Bohm to Pancharatnam–Berry and beyond, *Nat. Rev. Phys.* **1**, 437–449 (2019).

[7] E. Majorana Atomi orientati in campo magnetico variabile, *Nuovo Cimento* **9**, 43–50 (1932).

[8] R. Barnett, A. Turner, and E. Demler, Classifying novel phases of spinor atoms, *Phys. Rev. Lett.* **97**, 180412 (2006).

[9] R. Barnett, A. Turner, and E. Demler, Classifying vortices in $S = 3$ Bose-Einstein condensates, *Phys. Rev. A* **76**, 013605 (2007).

[10] H. Mäkelä, and K.-A. Suominen, Inert states of spin- s systems, *Phys. Rev. Lett.* **99**, 190408 (2007).

[11] E. Serrano-Ensástiga, and F. Mireles, Spinor Bose-Einstein condensates: self-consistent symmetries and

characterization, preprint arXiv:2211.16428 (2022).

[12] P. Mathonet et al., Entanglement equivalence of N -qubit symmetric states, *Phys. Rev. A* **81**, 052315 (2010).

[13] J. Martin, O. Giraud, P.A. Braun, D. Braun, and T. Bastin, Multiqubit symmetric states with high geometric entanglement, *Phys. Rev. A* **81**, 062347 (2010).

[14] M. Aulbach, D.J.H. Markham, and M. Murao, The maximally entangled symmetric state in terms of the geometric measure, *New J. Phys.* **12**, 073025 (2010).

[15] D.J.H. Markham, Entanglement and symmetry in permutation-symmetric states, *Phys. Rev. A* **83**, 042332 (2011).

[16] P. Ribeiro, and R. Mosseri, Entanglement in the symmetric sector of n qubits, *Phys. Rev. Lett.* **106**, 180502 (2011).

[17] M. Aulbach, Classification of entanglement in symmetric states, *Int. J. Quantum Inform.* **10**, 1230004 (2012).

[18] W. Ganczarek, M. Kuś, and K. Życzkowski, Barycentric measure of quantum entanglement, *Phys. Rev. A* **85**, 032314 (2012).

[19] A. Mandilara, T. Coudreau, A. Keller, and P. Milman, Entanglement classification of pure symmetric states via spin coherent states, *Phys. Rev. A* **90**, 050302(R) (2014).

[20] P. Hyllus, et al., Fisher information and multiparticle entanglement, *Phys. Rev. A* **85**, 022321 (2012).

[21] J.H. Hannay, The Berry phase for spin in the Majorana representation, *J. Phys. A: Math. Gen.* **31**, L53 (1998).

[22] P. Bruno, Quantum Geometric Phase in Majorana's Stellar Representation: Mapping onto a many-body Aharonov-Bohm Phase, *Phys. Rev. Lett.* **108**, 240402 (2012).

[23] H.D. Liu, and L.B. Fu, Berry phase and quantum entanglement in Majorana's stellar representation, *Phys. Rev. A* **94**, 022123 (2016).

[24] P. Ribeiro, J. Vidal, and R. Mosseri, Thermodynamical limit of the Lipkin-Meshkov-Glick model, *Phys. Rev. Lett.* **99**, 050402 (2007).

[25] P. Ribeiro, J. Vidal, and R. Mosseri, Exact spectrum of the Lipkin-Meshkov-Glick model in the thermodynamic limit and finite-size corrections, *Phys. Rev. E* **78**, 021106 (2008).

[26] J. Zimba, "Anticoherent" spin states via the Majorana Representation, *Electron. J. Theor. Phys.* **3**, 143 (2006).

[27] D. Baguette, T. Bastin, and J. Martin, Multiqubit symmetric states with maximally mixed one-qubit reductions, *Phys. Rev. A* **90**, 032314 (2014).

[28] O. Giraud, D. Braun, D. Baguette, T. Bastin, and J. Martin, Tensor representation of spin states, *Phys. Rev. Lett.* **114**, 080401 (2015).

[29] D. Baguette, F. Damanet, O. Giraud, and J. Martin, Anticoherence of spin states with point-group symmetries, *Phys. Rev. A* **92**, 052333 (2015).

[30] H.D. Liu, L.B. Fu, X. Wang, Coherent-state approach for Majorana representation, *Commun. Theor. Phys.* **67**, 611 (2017).

[31] D. Baguette, and J. Martin, Anticoherence measures for pure spin states, *Phys. Rev. A* **96**, 032304 (2017).

[32] P. Kolenderski, and R. Demkowicz-Dobrzański, Optimal state for keeping reference frames aligned and the Platonic solids, *Phys. Rev. A* **78**, 052333 (2008).

[33] C. Chryssomalakos, and H. Hernández-Coronado, Optimal quantum rotosensors, *Phys. Rev. A* **95**, 052125 (2017).

[34] A.Z. Goldberg, and D.F.V. James, Quantum-limited Euler angle measurements using anticoherent states, *Phys. Rev. A* **98**, 032113 (2018).

[35] J. Martin, S. Weigert, and O. Giraud, Optimal detection of rotations about unknown axes by coherent and anticoherent states, *Quantum* **4**, 285 (2020).

[36] J. Crann, D.W. Kribs, and R. Pereira, Spherical designs and anticoherent spin states, *J. Phys. A: Math. Theor.* **43**, 255307 (2010).

[37] E. Bannai, and M. Tagami, A note on anticoherent spin states, *J. Phys. A: Math. Theor.* **44**, 342002 (2011).

[38] M. Wang, and Y. Zhu, Anticoherent spin-2 states and spherical designs, *J. Phys. A: Math. Theor.* **55**, 425304 (2022).

[39] A.Z. Goldberg, A.B. Klimov, M. Grassl, G. Leuchs, and L.L. Sánchez-Soto, Extremal quantum states, *AVS Quantum Sci.* **2**, 044701 (2020).

[40] A.Z. Goldberg, M. Grassl, G. Leuchs, and L.L. Sánchez-Soto, Quantumness beyond entanglement: The case of symmetric states, *Phys. Rev. A* **105**, 022433 (2022).

[41] O. Giraud, P. Braun, and D. Braun, Quantifying quantumness and the quest for Queens of Quantum, *New J. Phys.* **12**, 063005 (2010).

[42] F. Bouchard, et al., Quantum metrology at the limit with extremal Majorana constellations, *Optica* **4**, 1429-1432 (2017).

[43] A. Tavakoli, and N. Gisin, The Platonic solids and fundamental tests of quantum mechanics, *Quantum* **4**, 293 (2020).

[44] H.Ch. Nguyen, S. Designolle, M. Barakat, and O. Gühne, Symmetries between measurements in quantum mechanics, preprint arXiv:2003.12553 (2022).

[45] J.I. Latorre, and G. Sierra, Platonic entanglement, *Quantum Inf. Comput.* **21**, 1081 (2021).

[46] K. Bolonek-Lasoń, and P. Kosiński, Groups, Platonic solids and Bell inequalities, *Quantum* **5**, 593 (2021).

[47] K.F. Pál, and T. Vértesi, Groups, Platonic Bell inequalities for all dimensions, *Quantum* **6**, 756 (2022).

[48] R. H. Dicke, Coherence in Spontaneous Radiation Processes, *Phys. Rev.* **93**, 99 (1954).

[49] G. Rajchel-Mieldzioć, Quantum mappings and designs, PhD thesis, preprint arXiv:2204.13008 (2022).

[50] R. Penrose, On Bell non-locality without probabilities: some curious geometry, *Quantum Reflections* (2000).

[51] J. Zimba and R. Penrose, On Bell non-locality without probabilities: More curious geometry, *Stud. Hist. Phil. Sci.* **24**, 697 (1993).

[52] J.E. Massad, and P.K. Aravind, The Penrose dodecahedron revisited, *Am. J. Physics* **67**, 631 (1999).

[53] J. Czartowski, D. Goyeneche, M. Grassl, and K. Życzkowski, Isoentangled Mutually Unbiased Bases, Symmetric Quantum Measurements, and Mixed-State Designs, *Phys. Rev. Lett.* **124**, 090503 (2020).

[54] D. Martin, and E.P. Wigner, Group theory and its application to the quantum mechanics of atomic spectra, *Academic Press Inc.* (1959).

[55] NCN Maestro 7 2015/18/A/ST2/00274 website https://chaos.if.uj.edu.pl/~karol/Maestro7/files/data3/Numerical_Results.dat